SEISMIC PERFORMANCE OF SINGLE-STORY PRECAST BUILDINGS: EFFECT OF CLADDING PANELS

Marianna ERCOLINO[1], Gennaro MAGLIULO[2], Gaetano MANFREDI[3]

Abstract: In reinforced concrete industrial precast structures one of the most common seismic damage is the collapse of the cladding panels because of the failure of the panel-to-structure connections. This damage is caused by the interaction between the panels and the structures, which is usually neglected in the design approach. The present study aims at investigating this interaction. Nonlinear dynamic analyses are performed on several structural models in order to take into account both the panel-to-structure interaction and the roof diaphragm. According to the analyses results, if the current European single-story precast buildings stock is considered, panels stiffness significantly influences the overall structural behavior under seismic actions and the failure of the connections occurs at very low intensity values. The progressive collapse of the panels is also simulated in order to evaluate the redistribution of seismic demand in the columns during the earthquake. In the final part, fragility curves are evaluated in order to generalize the dynamic analyses results.

Author keywords: precast structures, cladding panels, seismic response, dynamic analyses, incremental dynamic analysis, fragility curves

Introduction

Connection systems are the crucial points in the seismic performance of precast reinforced concrete (RC) structures. During recent earthquakes in Europe (Belleri et al., 2015, Belleri et al., 2014, Magliulo et al., 2014), several existing precast structures showed severe damage at the connections. One of the most common damage was the failure of the external cladding panels; it caused many injuries and casualties as well as significant economic losses due to the interruption of the industrial/commercial activities. The panels failure was caused by the connections fracture and it can be explained by the design approach. Indeed, the cladding panels are commonly considered as

[1] Senior Lecturer, University of Greenwich, Email: M.Ercolino@greenwich.ac.uk

[2] Assistant professor, University of Naples Federico II (corresponding author), E-mail: gmagliul@unina.it

[3] Full professor, University of Naples Federico II, E-mail: gamanfre@unina.it

26 nonstructural elements and the interaction with the structure under seismic loads is neglected.

27 According to Eurocode 8 (CEN, 2005), the panel-to structure connections are dimensioned only for

28 forces in the out-of-plane direction of the panels. These forces are both seismic actions deriving

29 from the panel self-weight and wind actions. However, under dynamic actions the panel-to-structure

30 interaction can occur and the connections could fail since they are carrying forces that were not

31 considered during the design phase, e.g. in-plane actions.

32 In the last decades several research studies were developed on the panel-to-structure interaction

33 under seismic loads. In these works the effect of the panels was investigated in order to evaluate

34 both the dynamic properties (e.g., frequencies and damping ratios) and the structural seismic

35 performance (e.g., drift ratios, displacement demand). However, most of these research studies

36 concerned some typical U.S. buildings, i.e. steel high-rise buildings, as extensively reported in Hunt

37 and Stojadinovic (2010). In the last years the scientific community recognized the need of a

38 systematic study on the structure-cladding panel interaction in RC precast buildings, typically

39 implemented in Europe for industrial and commercial activities. Recently, an European research

40 project was conducted on this topic: the SAFECLADDING project, aimed at studying the effect of

41 cladding panels on precast industrial buildings. In the framework of this project, a first study was

42 developed by Biondini et al. (2013); in this work the authors investigated the effect of vertical

43 panels by assuming the interaction at the level of the panel-to-panel connections. Since the

44 numerical forces in the connections were too high if the interaction between the panels was

45 considered, the authors proved the efficiency of an innovative dissipative connection between

46 vertical panels. In the framework of the same project, experimental campaigns were performed on

47 some typical panel-to-structure connection systems, in order to assess their seismic performance,

48 e.g. failure modes, strength and deformability (Zoubek et al., 2016). The experimental results were

49 used in order to perform a systematic seismic fragility study, described in Babič and Dolšek (2014).

50 In this research work, the authors performed 3D nonlinear analyses on several precast structures and

51 they defined the fragility curves for twelve industrial precast building classes. These classes were

52 defined by varying the type of non-structural components (vertical panels, horizontal panels and

53 masonry infills), the geometrical configuration, the design approaches and the panel-to-structure

54 connection systems. According to the outcomes of this study, the authors concluded that the effect

55 of non-structural components should be taken into account in both the design and the seismic

56 assessment of such buildings since the overall safety of the structures decreases if these components

57 are considered in the models. In this study the connection models are assumed from the

58 correspondent tested connections and the roof is modeled as flexible in its own plane. Despite the

59 noteworthy effort in the last years, other investigations are necessary in order to delineate more

60 general conclusions on the panel influence for precast structures as well as on the design of precast
61 structures with cladding panels. Indeed, during the design phase some simplified assumptions are
62 generally necessary (e.g., flexible or rigid roof hypotheses without modeling the roof elements in
63 the structural models). If the cladding panels have to be considered in the structural analysis, a
64 detailed model of the connections is required (e.g., based on experimental results), which should be
65 generalized by extensive experimental campaigns and/or numerical studies. At this aim, Magliulo et
66 al. (2015) proposed a simplified model of precast structure with cladding panels. In this model the
67 panel-to-structure interaction is assumed at the beam-to-panel connections (vertical panels), the
68 nonstructural elements are considered as elastic elements and the connections are fixed constraints
69 between the structure and the panel. By performing an extensive parametric study, the authors
70 evaluated the first periods of single-story precast buildings by means of linear modal analyses in
71 two limit cases: negligible panels effect (bare structures) and not-negligible panels effect (structures
72 with panels). In this last case, a significant effect of the panels on the structural dynamic behavior
73 was demonstrated and the simplified period formula of Eurocode 8 was compared with the analysis
74 results in order to verify its capability.

75 The presented study investigates the cladding panel effect on the nonlinear seismic response of a
76 reference precast industrial building. The adopted case-study is a new building, designed according
77 to Eurocodes. The seismic assessment of the structure is performed by means on nonlinear dynamic
78 analyses in OpenSees (McKenna and Fenves, 2013) program. Several structural models are
79 considered by varying the assumptions on both the roof stiffness and the occurrence of panel-to-
80 structure interaction. The results of models with the cladding panels demonstrate the significant
81 effect of the panels on the seismic behavior of these buildings; moreover, they justify the typical
82 connection failure under dynamic actions. In order to improve the reliability of the numerical
83 results, a model with the cladding panels is developed that is able to simulate the panel collapse
84 during the seismic load. If the panels collapse is simulated, the results show a significant difference
85 in the structural response in terms of both connection failure and forces distribution. In the final part
86 of the paper, the seismic vulnerability of the structures is evaluated by taking into account all the
87 above-cited modeling assumptions in order to define general conclusions to lead the designer to
88 choose the approach for such buildings.

89 **Case-study structure**

90 The investigated case study is a precast industrial building (Figure 1). It consists of precast
91 columns, fixed at the base by means of socket foundation and connected at the top by secondary
92 girders and principal beams in the two horizontal directions. The principal beams support the roof
93 elements. The columns height is equal to 9m (29.5 ft); the width of the six X-bays is 12m (39.4 ft)

and the width of the two Z-bays is 19m (62.3 ft). The horizontal elements are designed by considering only the vertical loads (permanent and variable loads); they consist of prestressed TT roof elements, prestressed principal beams in the transversal direction (Z direction in Figure 1) and secondary girders in the longitudinal direction (X direction in Figure 1). Dowel connections are usually installed between the principal beam and the columns as well as between the roof elements and the principal beams. The girder-to-column connection usually consists of bolted steel joints. Vertical reinforced concrete precast cladding panels are connected to beams or girders, as described in section "Model with cladding panels".

The columns are designed according to Eurocode 8 (CEN, 2005), assuming a peak ground acceleration equal to 0.168g (return period of 475 years and soil type "B") and ductility class "DCH". The behavior factor is equal to 4.5, as indicated in Eurocode 8. The columns have square-shaped cross-sections (80cm x 80cm – 31.5 inches x 31.5 inches) reinforced with 22mm diameter longitudinal bars (ρ=1.66%) and 10mm (0.39 inches) diameter stirrups, 12.5cm (4.9 inches) spaced. The concrete cubic characteristic strength is equal to 55N/mm^2 with an elastic modulus equal to 36283N/mm^2 (757786 kips/ft^2), computed according to Eurocode 2 (CEN, 2004). The reinforcement steel has a yielding characteristic strength equal to 450N/mm^2 (9398 kips/ft^2).

The total seismic weight is equal to about 6.7kN/m^2 (140 kips/ft^2). The design is performed, as usually happens, assuming bare structure and rigid diaphragm.

The design fundamental periods along the two horizontal directions of the designed structure are equal to 1.2sec.

Nonlinear models

Nonlinear dynamic analyses are performed in OpenSees (McKenna et al., 2013) software on six structural models by taking into account P-Δ effects. In order to investigate the panel effect, three models are defined: the bare structure and two different models for the building with cladding panels. Moreover, the three models are investigated by assuming two different hypotheses: either the rigid roof in its own plane hypothesis (RF) or the flexible roof (FR) hypothesis. In the former case, the seismic mass of the structures is concentrated in the mass barycenter and the roof is modelled as a rigid body in its own plane. In the latter case, the masses are concentrated at the columns top and no constraints are considered for the roof. In the model with the simulated collapse, the mass of the panels is concentrated in the beam-to-panel connection points in order to remove such mass if the panel collapses during the dynamic analysis.

Concerning the connections between the structural elements, the beam-to-column connections are dowel systems and they can be assumed as hinges. Therefore, the columns carry the horizontal seismic actions and the horizontal elements sustain only the vertical loads.

128 The fundamental periods along the two horizontal directions of the six structural models are
129 reported in Table 1. It is worth noting that the periods of the bare model are larger than the
130 corresponding periods of the design model, because the secant stiffness to the yielding point of the
131 nonlinear bare model is lower than the assumed elastic stiffness of the design model.

132 ### *Bare model*

133 In the bare model (BM) the panel-to-structure interaction is neglected; the model consists of
134 columns, girders and principal beams. This assumption is the common modeling approach adopted
135 for precast structures: the panels do not take part to the global structural response under seismic
136 actions.

137 The nonlinear response of the structure is concentrated at the columns base by means of a lumped
138 plasticity approach and the horizontal elements are assumed elastic one-dimensional elements. A
139 tri-linear moment-rotation envelope is assigned to the plastic hinge, consisting of three
140 characteristic points: yielding, capping and post-capping points. The envelope points are assumed
141 according to Fischinger et al. (2008). The yield drift is calculated according to the formula proposed
142 by Fardis and Biskinis (2003):

143 $$\theta_y = \phi_y \cdot L_s / 3 + 0.00275 + a_{sl} \cdot \frac{\varepsilon_y}{d - d'} \cdot \frac{0.2 \cdot d_b \cdot f_y}{\sqrt{f_c}} \tag{1}$$

144 The yield curvature (ϕ_y) is evaluated according to the bi-linearization of the moment-curvature
145 envelope, obtained by a fiber analysis of the column cross-section. In the fiber analysis three types
146 of fibers are considered in the cross-section: the unconfined concrete fibers in the concrete cover;
147 the concrete confined fibers (Mander et al., 1988) in the concrete core and the steel fibers of the
148 reinforcing bars. The median values of both the concrete compressive strength (f_c=53N/mm^2 -
149 1107 kips/ft^2) and the steel yielding strength (f_y=530N/mm^2 - 11069 kips/ft^2) are defined according
150 to Eurocode 2 (CEN, 2004). The slip coefficient (a_{sl}) is assumed equal to 1 and the term *(d-d')* is
151 evaluated as the distance between the tension and compression reinforcement. According to the
152 structural scheme, the shear span (L_s) is equal to the height of the column. In Eq. (1) the ε_y is the
153 yielding strain of the reinforcement (0.21%) and d_b is the diameter of the longitudinal reinforcement
154 (22mm – 0.87 inches).

155 The capping and post-capping rotations are evaluated according to Haselton (2006):

156 $$\theta_{cap} = 0.12 \cdot \left(1 + 0.4 \cdot a_{sl}\right) \cdot 0.2^V \cdot \left(0.02 + 40 \cdot \rho_{sh}\right)^{0.52} \cdot 0.56^{0.01 f_c} \cdot 2.37^{10.0\rho} \tag{2}$$

157 $$\theta_{pc} = 0.76 \cdot 0.031^V \cdot \left(0.02 + 40 \cdot \rho_{sh}\right)^{1.02} \leq 0.1 \tag{3}$$

158   In Equations (2) and (3) ν is the normalized axial force, ρ_{sh} is the transverse reinforcement ratio and

159   ρ is the longitudinal reinforcement ratio. Given the yielding moment (M_y) by the bi-linearization of

160   the moment-curvature curve, the capping moment (M_c) is determined as:

161    $$M_c\big/M_y = 1.25 \cdot 0.89^\nu \cdot 0.91^{0.01 \cdot f_c} \tag{4}$$

162   The energy dissipation capacity of the plastic hinge is taken into account by the factor λ (Eq. (5)),

163   according to Ibarra et al. (2005).

164    $$\lambda = 127.2 \cdot 0.19^\nu \cdot 0.24^{s/d} \cdot 0.595^{V_p/V_n} \cdot 4.25^{\rho_{sh,eff}} \tag{5}$$

165   In Eq. (5) s/d is the ratio between the stirrup spacing (12.5cm – 4.9 inches) and column depth

166   (80cm – 31.5 inches); V_p/V_n is the ratio between the shear at flexural yielding and the shear

167   strength; and $\rho_{sh,eff}$ is the effective ratio of transversal reinforcement.

168   Figure 2 shows the envelopes of the three adopted plastic hinges, corresponding to columns

169   characterized by different values of the axial force: A) internal columns (gray marker in Figure 2b),

170   B) perimetral columns (blue marker in Figure 2b) and C) corner columns (black marker in Figure

171   2b). This terminology and the colors in Figure 2b are adopted in the following section in order to

172   individuate the columns in the structure.

173

174   ***Model with cladding panels***

175   In the Model With Panels (MWP) the cladding panels are introduced in order to take into account

176   their interaction with the structure. The structural elements (columns, girders and beams) are

177   modelled as in the BM. In this study, the vertical panels are investigated and the connection at the

178   top is shown in Figure 3. The connection at the bottom of the panel may consist of clip-panel beams

179   equipped with a fork or welded/bolted metal anchors. The adopted model does not consider the

180   uplift capacity of the panel at the bottom. Each panel consists of an elastic 2D frame (Figure 4) and

181   it is connected at the top to the structure (beam) by means of fixed constraints that avoid the panel-

182   to-structure relative displacement (Magliulo et al., 2015), as often shown during recent earthquakes

183   (Magliulo et al., 2014). The influence of a more detailed model of the panel-to-structure connection

184   will be investigated by the authors in a future research study. Preliminary studies on a single bay

185   structure show that the assumption of rigid connection causes an underestimation of the collapse

186   fragility.

Model with progressive collapse

In order to simulate the panel collapse, a model (MR) is introduced in OpenSees. This model simulates the panel collapse by means of the "Removal" command (Talaat and Mosalam, 2009). Such a model can be used in order to achieve three main purposes:

> i) the evaluation of the real forces at the base of the structural elements during an earthquake;
>
> ii) the justification of the recorded damage in the structural elements due to a seismic event after the collapse of the cladding panels;
>
> iii) the vulnerability assessment of precast single-story structures.

The "Removal" command allows removing from the structural model the cladding panels that achieve the maximum strength in the connection system during the nonlinear dynamic analysis, i.e. once the collapse of the connection is achieved, the analysis of the structure continues without the corresponding panel. In this study, only the shear failure of the connector is considered (Figure 3). Each panel is characterized by two connections with the structure at the top and for each connection a limit domain is defined in terms of displacements in the two horizontal directions. For the out of the plane actions, a very large limit displacement is assumed; on the contrary, for the in-plane direction the limit displacement is evaluated according to the shear strength of the connector. These assumptions are justified by the design approach, typically adopted for panel-to-structure connection in precast buildings (see "Introduction").

Input

Bi-directional nonlinear dynamic analyses are performed with both the components of 7 natural seismic events (CEN, 2005). In Table 2 the main parameters of the selected natural earthquakes are reported in terms of: earthquake ID, name of the real event, date of the event, magnitude, peak ground acceleration in horizontal X and Y direction and type of soil according to the EC8 categories. The records selection was performed by the software REXEL (Iervolino et al., 2010) in order to match the design elastic spectrum of the considered site with all the 14 records (see Section Case-study structure). Figure 5 shows the comparison between the mean spectrum of the selected records and the design spectrum at a return period of 475 years; in this figure the spectra of the records are reported for the two horizontal components, corresponding to the X (solid lines) and Z (dashed lines) directions in this study. The dispersion of the spectral acceleration for the selected ground motions is justified by the need of ensuring the spectrum compatibility for a wide range of periods. Such a need is required to cover both bare structures and structures with cladding panels (Magliulo et al., 2015).

Nonlinear analyses results

The seismic response of precast structures is investigated by means of nonlinear dynamic analyses in OpenSees, considering the above-described structural models. In order to simplify the discussion about the results, Table 3 shows an overview of the adopted structural models and it introduces the corresponding symbols adopted in the following.

The structural safety is investigated for the Near Collapse Limit State (NC LS). It is assumed to be achieved when 20% decay of the maximum strength occurs in the first plastic hinge (Fischinger et al., 2008). According to this criterion, the rotational capacity of the plastic hinges are equal to the following values: 1) 0.0850 for internal columns, 2) 0.0768 for perimetral columns and 3) 0.0785 for corner columns. In the model with cladding panels, the safety of the connections is also verified in terms of shear strength of the connector.

Bare models

This section shows the results of the nonlinear dynamic analyses on the bare models. The results of the bare model with rigid roof (BM-RR) are shown in Figure 6; the moment-rotation envelopes of all the columns of the structure are reported around the Z (Figure 6a) and X (Figure 6b) directions, for all the seismic events: for each type of column (perimetral, internal and corner), the moment-rotation diagram with the maximum rotation is shown. Around both the directions the columns have an elastic response (i.e., the maximum rotation is lower than the assumed yielding rotation) under all the seismic ground motions; however, around X direction the columns reach the capping rotation for one record (ID=535). This result is justified by the large spectral acceleration (Figure 5b) of this seismic event at the period of the structure (1.60sec). According to the adopted criterion, the structure is safe with respect to the NC LS for all the records.

The recorded elastic response demonstrates a significant overstrength of the considered benchmark structure. This overstrength is caused by several reasons, such as the difference between the stiffness of the structures assumed in the design phase and in the dynamic analysis and the difference between the medium and the design values of the material mechanical characteristics. For instance, the yielding force assumed in the nonlinear analysis seismic force of each column is twice the design seismic force of each column. It is interesting to note that this overstrength occurred besides some design aspects: 1) the assumed high value of the behavior factor (q=4.5) and 2) the percentage of longitudinal reinforcement that is higher than the minimum percentage required by the code (ρ=1.0%). According to these two considerations, the overstrength of the structure should not be high and an inelastic behavior would be expected under a set of earthquakes matching the elastic design spectrum. This conclusion on the seismic safety/overstrength of the precast

253   structures should be validated by taking into account also the variability in the seismic action and

254   materials (Fischinger et al., 2009).

255   If the flexible roof is considered in the bare model (BM-FR), the response is still elastic for the most

256   of the records (Figure 7). However, the rotational demand increases in both perimetral and internal

257   columns due to the higher value of relevant masses. It is worth highlighting the distribution of

258   seismic demand in the structural frames. Figure 8 shows the demand/capacity ratios in terms of

259   rotations for two external frames around X and Z direction. The markers are reported for all the

260   adopted records. The different seismic demand on the columns as well as on the frames

261   demonstrates the absence of the rigid diaphragm; in this case, the distribution of seismic demand

262   can significantly change throughout the columns and it can lead to a low ductile behavior of the

263   overall structure. However, the NC LS is not attained, since the median value (red lines) of the

264   demand/capacity ratios is lower than one. The results in the other frames and in Z direction are not

265   showed for the sake of brevity.

266   ### *Structures with panels*

267   Nonlinear dynamic analyses are performed on the models with cladding panels (MWP) with the

268   same set of records. The results are presented in terms of distribution of forces in the structural

269   elements and in the connection system with the rigid (RR) and the deformable roof (FR)

270   hypotheses.

271   Figure 9 shows the moment-rotation curve around X and Z direction of the columns for the MWP-

272   RR: the behavior is elastic and the seismic demand in the columns is very low because of the high

273   stiffness of the cladding panels. If the flexible roof is assumed (MWP-FR), the seismic demand in

274   the columns significantly increases and the behavior is quite similar to the BM-FR (Figure 10). In

275   the case of the flexible roof the stiffness of the panels does not influence the seismic demand in the

276   columns.

277   In order to assess the seismic safety of the panel-to-structure connections, the shear demands are

278   compared to the shear strength of a typical connection. The design of this connection is performed

279   according to the above-described design approach: the seismic design forces are evaluated by

280   considering only the weight of the panel and they are applied in the out of plane direction. Figure 11

281   shows the comparison between the demand from the analysis and the shear strength of the

282   connection for the MWP-RR. In particular, in this figure the markers indicate the demand/capacity

283   ratios in terms of shear of the connector (CEN, 2005) in the panel direction (Figure 11a in X

284   direction and Figure 11b in Z direction) for each record and for the panels in one frame. In both the

285   directions, the shear strength of the connector is smaller than the seismic forces in the connection.

286 If the deformable roof is assumed (MWP-FR), the seismic forces in the panel-to-structure
287 connections significantly decrease (Figure 12). This result agrees with the above-presented
288 moment-rotation curves and it is related to the floor in plane deformability: larger forces are
289 recorded in the internal frames because of their larger relevant seismic masses.

290 The results of the nonlinear dynamic analyses justify the widespread failures of cladding panels
291 during some recent earthquakes in Europe. In both the models (i.e., RR and FR) the large stiffness
292 of these nonstructural components causes a significant reduction of the seismic forces in the
293 structural elements (columns) as well as large forces at the panel-to-structure connections. The
294 magnitude of these forces is significantly larger than the strength of the connection, i.e. the shear
295 strength of the connector in the in-plane direction of the panel.

296 ***Progressive collapse***

297 The results of the nonlinear dynamic analyses have demonstrated the vulnerability of the panel-to-
298 structure connections if the panels interact with the structure under seismic actions. The low
299 demand/capacity ratios justify the collapse of the panels in the early steps of a seismic record, i.e.
300 also for very low values of acceleration. During the time-history, the collapse of the panels leads to
301 a change of the stiffness distribution in the structures (i.e., change in the dynamic properties) as well
302 as a different seismic demand in the structural elements (columns). In order to investigate such a
303 behavior, nonlinear dynamic analyses are performed on MR-RR and on MR-FR.

304 Figure 13 shows the model capability by reporting two steps of one nonlinear dynamic analysis on
305 MR-RR: in the first steps few panels have collapsed (Figure 13a); whereas in the final step the most
306 of the panels have collapsed under the seismic records (Figure 13b). Figure 14 shows the moment-
307 rotation curves around the two horizontal directions for MR-RR: the structure has an elastic
308 response under all the adopted records; however, the forces increase with respect to the model with
309 cladding panels (MWP-RR, see Figure 9). For instance, in this model the yielding rotation is
310 achieved around X direction for record ID=575.

311

312 If the deformable roof is considered (RM-FR) the following conclusions can be drawn by means of
313 the moment-rotation curves in Figure 15.

314   - Around X direction, the columns experience rotations that are similar to the results in the
315   MWP-FR. In this model the distribution of the seismic demand is influenced by the mass
316   distribution: the internal columns are bearing larger forces than the external ones in both the
317   models. However, the demand on the corner columns increases because of the collapse of
318   the panels during the analysis (Figure 16a).

319   -   Around Z direction, the maximum recorded rotations in the RM are larger than the
320   maximum values in the MWP for the corner columns. The collapse of the panels during the
321   analysis causes an irregular distribution of masses and stiffness in the structure and,
322   therefore, torsional modes can significantly influence the seismic demand in the columns.
323   -   For some records (n.535 and n.196) the rotations around Z direction are significantly larger
324   than in the MWP-FR. In the case of the removal model the collapse of some of the panels
325   causes large changes of the fundamental periods. At the beginning of the analysis, the
326   periods are equal to the model with cladding panels (MWP, see Table 1) as well as the
327   seismic demand. Whereas during the analysis the period increases due to the reduction of
328   the structural stiffness (periods close to the ones of the model BM) and the seismic demand
329   increases for the earthquakes n.535 and n.196 (Figure 5). Figure 16 shows a clear
330   comparison between the results of the analyses on the two models for corner columns
331   around Z direction.
332   -   A very similar conclusion can be stated by comparing the results of the RM-FR (Figure 15)
333   and the results of the BM-FR (Figure 7). The behavior of the RM is very similar to the BM
334   because of the panels collapse in the early steps of the time-histories. For some records the
335   smaller rotations in the BM can be justified because the values of the spectral acceleration at
336   T=1.6sec (e.g., at the period of the BM) are lower than the values of the spectral
337   acceleration at the periods of the RM (in the range 0.5-1.0sec).

338
339

340 **Fragility curves**
341 A seismic risk study is performed on the investigated benchmark structure in order to define the
342 fragility curves for different structural modeling assumptions. The fragility curves are defined for
343 predicting the probability of exceeding a certain level of performance in the structure. In this study,
344 the global collapse limit state of the structure is considered, i.e. the condition in which a structural
345 system is unable to support vertical loads when subjected to seismic excitation.

346 *Incremental dynamic analyses*
347 In order to evaluate the limit state capacity of the structure, incremental dynamic analyses (IDA) are
348 performed (Vamvatsikos and Cornell, 2002). The IDA curves are defined by adopting as Intensity
349 Measure (IM) the peak ground acceleration and as Damage Measure (DM) the roof displacement.
350 The adopted DM is evaluated as the square-root-sum-of-squares of the instantaneous drifts in the
351 two principal directions (Vamvatsikos, 2006, Wen and Song, 2003)

352 In order to assess the global collapse performance in the structure the IM-based rule is adopted: it

353 defines a single point on each IDA curve that corresponds to the achievement of the global collapse

354 limit state. In particular, in this work the collapse criterion is defined by the achievement of a

355 stiffness equal to 20% of the elastic one (FEMA, 2000). This criterion corresponds to consider the

356 flattening of the curve as an indicator of the dynamic instability, i.e. an indicator of collapse

357 (Fischinger et al., 2009). In the case of the models with cladding panels (MWP), the collapse of the

358 structure can be also achieved if the panels fail, i.e. the seismic demand in the panel-to-structure

359 connections achieves the shear strength of the connector.

360 The nonlinear analyses are performed with a set of twenty-two ground motion record pairs from

361 sites located greater than or equal to 10km from fault rupture, referred to as the "Far-Field" in

362 FEMA (2008). The record set includes records from all large-magnitude events in the PEER NGA

363 database (PEER, 2006). Figure 17 shows the spectra of the adopted records, scaled to PGA=1g.

364 ### *Results*

365 In this section the results of the seismic risk study are presented for all the considered models (bare,

366 with cladding and with removal) and with the two hypotheses on the roof stiffness (rigid and

367 flexible behavior). The considered IM is the peak ground acceleration.

368 Figure 18 and Figure 19 show the IDA curves evaluated for the BM-RR and the BM-FR,

369 respectively. In the same figure the lognormal distribution of the collapse IMs is also reported (red

370 area). The mean value of the peak ground acceleration at the collapse lightly change in the two

371 models; therefore, the fragility curves for the two modeling approaches are similar (Figure 20).

372 The incremental dynamic analyses are also performed on the models MWP-RR and MWP-FR. In

373 the following the results are reported in terms of IDA curve and PDF distribution (Figure 21 and

374 Figure 22). For all the records, the collapse corresponds to the attainment of the shear strength in

375 the connection system, i.e. the shear failure of the connector occurs before the global collapse of the

376 structure. The results highlight the effect of the panels on the seismic risk of the considered precast

377 structure. If the deformable roof is considered the mean peak ground acceleration at the global

378 collapse is significantly larger than in the rigid roof case (Figure 22). This evidence confirms the

379 effect of the mass distribution to the response of the structure: the external frame are carrying

380 smaller forces because of the smaller mass. Figure 23 shows the fragility curves for the structures

381 with cladding panels: the hypothesis on the roof behavior significantly influences the safety of the

382 structure as well as the correspondent seismic risk. The failure criterion in the structures with

383 cladding panels corresponds to the failure of the first panel connection. In this case, the failure of

384 this non-structural element corresponds to the failure of the structure because it can cause danger

385   for the human life. The results of this analysis can highlight the significant seismic vulnerability of
386   the panel connections.
387   If the collapse of the panels is simulated in the models (RM-RR and RM-FR), the IDA curves are
388   showed in Figure 24 and in Figure 25. The failure criterion is defined at the failure of the columns
389   at the base (dynamic instability). In this case the mean collapse IM is very similar to the values of
390   the bare modes. Figure 26 shows the fragility curves for these structural models. The median value
391   of the IM at collapse in the removal models (1.42g and 1g for RR and FR, respectively) is more
392   similar to the values of the corresponding bare models (1.75g and 1.47g for RR and FR,
393   respectively) than to the values of the models with cladding panels (0.006g and 0.0235g for RR and
394   FR, respectively). The collapse of the panels occurs in the very early stage of the seismic records
395   due to the low shear strength of the connectors; during the transient part of the input the structure is
396   behaving like a bare system. It is worth to highlight that the bare models are not on the safe side in
397   the evaluation of the collapse IM of this structure. The results of the two models (BM and RM) can
398   be compared in order to justify the typical modelling assumption of neglecting the presence of
399   cladding panels during both the design and safety assessment phases.
400   The values of the collapse peak ground acceleration are quite larger than the values found in Dolsek
401   et al. (2016): this evidence can be justified by some reasons, such as: 1) the investigated buildings
402   are designed for different building codes; 2) in the work by Dolsek et al. (2016) the collapse of the
403   structure could be achieved by the failure of the dowel connections between the columns and the
404   beams; on the contrary, in the presented paper a strong connection is assumed.

405   **Conclusions**
406   This work aims at defining the effect of the cladding panels on the seismic response of RC single-
407   story precast structures. Such effect is evaluated by comparing the results of nonlinear dynamic
408   analyses on six structural models, i.e. by neglecting the interaction between the panel and the
409   structure (bare models) and by modeling the panel-to-structure interaction; in this last case two
410   conditions are taken into account: panel-to-structure interaction staying till the analysis end (models
411   with cladding panels) and progressive panel collapse simulation (removal models). For each model
412   both the rigid and the flexible roof in its own plane hypotheses are considered.
413   The results of the analyses on the bare structures highlight some main conclusions.
414   -   The effect of the rigid roof is negligible; however, the seismic performance gets worse if the
415   flexible roof is considered, because the seismic demand is not uniformly distributed in the
416   structural elements.
417   -   The overstrength of the structure leads to an elastic behavior under seismic actions and it is
418   mainly caused by the design assumptions in terms of stiffness and material strength.

419   In the case of the model with cladding panels, the following conclusions can be drawn.

420   -   The structural performance significantly changes with respect to the bare model if the roof is
421   rigid. In this case, the large stiffness of the panels causes a low demand on the structural
422   elements as well as a significant change in the dynamic properties of the structures.

423   -   In the case of the model with panels and rigid roof, the large forces at the panel-to-structure
424   connections justify the early collapse of the connections during the seismic events. The
425   demand is much larger than the shear strength of the connection in the direction of the panel.
426   The assumption of these connections as rigid constraints under dynamic actions is justified
427   by their behavior observed during recent earthquakes.

428   -   If the model with cladding panels provides the deformable roof, the seismic response of the
429   structures changes as well as the seismic demand at the panel-to-structure connections. The
430   seismic demand on the internal columns increases since the seismic forces distribution is
431   based on the seismic masses rather than on the stiffness of the structural elements. For the
432   same reason, the seismic demand on the connections of the panels decreases.

433   The analyses on the model with panels demonstrate that the panel-to-structure connections fail in
434 the very early stages of the seismic input (low intensity seismic level). In order to investigate the
435 real behavior of the structures during an earthquake, a novel model is developed (removal model).
436 This model allows recording the redistribution of the forces during a time-history in all the
437 structural elements by simulating the progressive collapse of the panels. The results of the nonlinear
438 dynamic analyses demonstrate that the forces in the columns increase as the panels fail and the
439 overall behavior of the structure is very similar to the behavior of the bare structures. This model
440 might simulate the failure of precast structures, occurred during some seismic events after the
441 collapse of the panels.

442   In the final part, a seismic risk study is performed in order to define the fragility curves of all the
443 investigated modeling approaches.

444   -   If the flexibility of the roof is considered, the mean peak ground acceleration values lightly
445   decreases at the collapse because of the irregular distribution of the seismic demand in the
446   structural elements. However, in both the bare models, the large values of the mean peak
447   ground acceleration highlight the overstrength of the structure.

448   -   If the panel-to-structure interaction is considered, the failure of the structures occurs for very
449   low values of the peak ground acceleration for both the models with cladding panels. The
450   results are significantly influenced by the assumption on the failure criteria: for all the
451   records the failure is achieved at the collapse of the panel connection. If the roof is rigid in
452   its own plane, the peak ground acceleration at the collapse is very low.

453   - If the progressive collapse of the panels is simulated, the fragility analysis gives results
454   similar to the bare model. This evidence demonstrates that the panel-to-structure
455   connections fail for very low seismic intensities (early stages of the seismic event); in this
456   case, the structural behavior is not significantly affected by the panels. However, the overall
457   behavior of the bare model does not predict a safe-sided behavior: the collapse of the bare
458   structure occurs for a seismic intensity that is larger (20% for rigid roof and 50% for flexible
459   roof) than the value with the panel progressive collapse.

460   The influence of a more detailed model of the panel-to-structure connection will be investi-
461   gated by the authors in a future research study. It should be underlined that the above presented
462   conclusions and results are limited to one-story precast buildings with strong connection
463   systems.

469 **References**

470   Babič, A., and Dolšek, M. "The impact of structural components on fragility curves of single-storey

471   industrial precast structures." *Proc., Second European conference on earthquake engineering and*

472   *seismology*, Istanbul, Turkey.

473   Belleri, A., Brunesi, E., Nascimbene, R., Pagani, M., and Riva, P. (2015). "Seismic Performance of

474   Precast Industrial Facilities Following Major Earthquakes in the Italian Territory." *Journal of*

475   *Performance of Constructed Facilities*, 29(5), 04014135.

476   Belleri, A., Torquati, M., and Riva, P. (2014). "Seismic performance of ductile connections between

477   precast beams and roof elements." *Mag Concrete Res*, 66, 553-562.

478   Biondini, F., Dal Lago, B., and Toniolo, G. (2013). "Role of wall panel connections on the seismic

479   performance of precast structures." *B Earthq Eng*, 11(4), 1061-1081.

480   CEN (2005). "Design of steel structures. Part 1-8: Design of joints." *Eurocode 3*, Brussels.

481   CEN (2005). "Design of structures for earthquake resistance, part 1." *Eurocode 8*, Brussels.

CEN (2004) "Eurocode 2: Design of concrete structures - Part 1-1: General rules and rules for buildings." *Eurocode 2*, Brussels.

Fardis, M. N., and Biskinis, D. (2003). "Deformation capacity of RC members, as controlled by flexure or shear." International Symposium on Performance-based Engineering for Earthquake Resistant Structures, University of Tokyo.

FEMA (2000). "Recommended seismic design criteria for new steel- moment frame buildings." Federal Emergency Management Agency, Washington.

FEMA (2008). "ATC-63 Project Report: Quantification of Building Seismic Performance Factors." Federal Emergency Management Agency, Washington.

Fischinger, M., Kramar, M., and Isakovic, T. (2009). "Seismic safety of prefabricated reinforced-concrete halls - analytical study." *Gradev*, 61(11), 1039-1045.

Fischinger, M., Kramar, M., and Isaković, T. (2008). "Cyclic response of slender RC columns typical of precast industrial buildings." *Bull. Earthq. Eng.*, 6(3), 519-534.

Haselton, C. (2006). *Assessing Seismic Collapse Safety of Modern Reinforced Concrete Moment-Frame Buildings*, PEER Report, Department of Civil Engineering California State University, Chico.

Hunt, P. J., and Stojadinovic, B. (2010). *Seismic Performance Assessment and Probabilistic Repair Cost Analysis of Precast Concrete Cladding Systems for Multistory Buildings*, Pacific Earthquake Engineering Research Center, College of Engineering, University of California, Berkeley.

Ibarra, L. F., Medina, R. A., and Krawinkler, H. (2005). "Hysteretic models that incorporate strength and stiffness deterioration." *Earthq Eng Struct D*, 34(12), 1489-1511.

Iervolino, I., Galasso, C., and Cosenza, E. (2010). "REXEL: computer aided record selection for code-based seismic structural analysis." *Bull. Earthq. Eng.*, 8(2), 339-362.

Magliulo, G., Ercolino, M., and Manfredi, G. (2015). "Influence of cladding panels on the first period of one-story precast buildings." *Bulletin of Earthquake Engineering*, 13(5), 1531-1555.

507 Magliulo, G., Ercolino, M., Petrone, C., Coppola, O., and Manfredi, G. (2014). "The Emilia

508 Earthquake: Seismic Performance of Precast Reinforced Concrete Buildings." *Earthq Spectra*,

509 30(2), 891-912.

510 Mander, J. B., Priestley, M. J. N., and Park, R. (1988). "Theoretical Stress-Strain Model for

511 Confined Concrete." *J. Struct. Eng.-Asce*, 114(8), 1804-1826.

512 McKenna, F., and Fenves, G. (2013). "OpenSees Manual http://opensees.berkeley.edu." *Pacific*

513 *Earthquake Engineering Research Center*.

514 PEER (2006). "PEER NGA Database http://peer.berkeley.edu/nga/." PEER Center, College of

515 Engineering, University of California.

516 Talaat, M., and Mosalam, K. M. (2009). "Modeling progressive collapse in reinforced concrete

517 buildings using direct element removal." *Earthquake Eng Struc*, 38(5), 609-634.

518 Vamvatsikos, D. "Incremental dynamic analysis with two components of motion for a 3D steel

519 structure." *Proc., 10th International Conference on Applications of Statistics and Probability in*

520 *Civil Engineering*,Tokyo.

521 Vamvatsikos, D., and Cornell, C. A. (2002). "Incremental dynamic analysis." *Earthq Eng Struct D*,

522 31(3), 491-514.

523 Wen, Y., and Song, S. (2003). "Structural Reliability/Redundancy under Earthquakes." *Journal of*

524 *Structural Engineering*, 129(1), 56-67.

525 Zoubek, B., Fischinger, M., and Isaković, T. (2016). "Cyclic response of hammer-head strap

526 cladding-to-structure connections used in RC precast building." *Engineering Structures*, 119, 135-

527 148.

528

529

530 **Table 1 Fundamental periods of the six structural models [sec]**

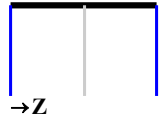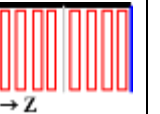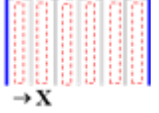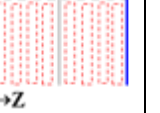|	Bare Model		With panels (WP)		Removal (R)	
	Rigid	Flexible	Rigid	Flexible	Rigid	Flexible
T1	1.62	1.70	0.15	1.63	0.15	1.63
T2	1.58	1.64	0.12	1.62	0.12	1.60
T3	1.35	1.41	0.08	1.52	0.08	1.52

531

532
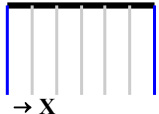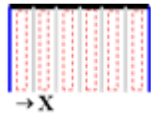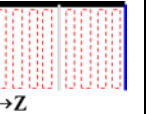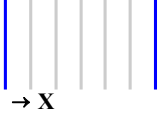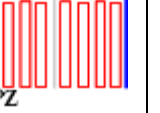
533   **Table 2** Features of the selected seismic events

ID	Earthquake Name	Date	M_w	PGA_x [g]	PGA_y [m/s²]	EC8 Site class
134	Friuli (aftershock)	15/09/1976	6.0	0.25	0.21	
147	Friuli (aftershock)	15/09/1976	6.0	0.13	023	
196	Montenegro	09/04/1979	6.9	0.44	0.29	
231	Montenegro (aftershock)	24/05/1979	6.2	0.16	0.13	B
291	Campano Lucano	23/11/1980	6.9	0.15	0.17	
535	Erzincan	13/03/1992	6.6	0.38	0.50	
1714	Ano Liosia	07/09/1999	6.0	0.23	0.21	

534

535

536 **Table 3** Overview of the adopted structural models

Roof (R)	Structural model (M)		
	Bare (B)	With panels (WP)	Removal (R)
Rigid (R)	→X →Z	→X →Z	→X →Z
Flexible (F)	→X →Z	→X →Z	→X →Z

537